mathematics

MDPI

Article

Finite Element Analysis of Generalized Thermoelastic Interaction for Semiconductor Materials under Varying Thermal Conductivity

Aatef Hobiny [1] and Ibrahim Abbas [1,2,*]

[1] Mathematics Department, Faculty of Science, King Abdulaziz University, Jeddah 21589, Saudi Arabia
[2] Mathematics Department, Faculty of Science, Sohag University, Sohag 82524, Egypt
* Correspondence: ibrabbas7@science.sohag.edu.eg

Abstract: In this work, we consider the problem of a semiconductor half-space formed of varying thermal conductivity materials with and without Kirchhoff's transforms. Specifically, we deal with one thermal relaxation time within the context of generalized photothermoelastic theory. It is expected that the thermal conductivity of the material will vary with temperature. The finite element method is used to numerically solve this problem. The Laplace transform and the eigenvalues method are used to determine analytical solutions to the linear problem. Various hypotheses are investigated, both with and without the use of Kirchhoff's transformations, to consider the influence of thermal conductivity change. To verify the accuracy of the proposed approach, we provide a comparison of numerical and analytical results by ignoring the new parameters and investigating the behaviors of physical quantities for numerical outcomes.

Keywords: finite element method; variable thermal conductivity; semiconductor materials; thermal relaxation time

MSC: 35Q81

Citation: Hobiny, A.; Abbas, I. Finite Element Analysis of Generalized Thermoelastic Interaction for Semiconductor Materials under Varying Thermal Conductivity. *Mathematics* **2022**, *10*, 4676. https://doi.org/10.3390/math10244676

Academic Editor: Ramoshweu Solomon Lebelo

Received: 16 November 2022
Accepted: 6 December 2022
Published: 9 December 2022

1. Introduction

The versatility of semiconducting materials in modern technology makes them a vital topic for study in the sciences. Most of these studies concentrate on investigating various forms of renewable energy. Semiconductors are a model for the utilization of renewable energy when they are exposed to sunshine. Neither the internal structures of these materials when subjected to external fields and activated by a laser beam, nor the link between thermal conductivity and temperature were considered in most previous experiments. Deformations during the microinertia of the microelement contribute to the body's temperature rise, in addition to external and internal thermal causes. In many of these uses [1], the effects of sunlight or laser beams on the surface of semiconductors materials are examined without considering the media's internal structures. Different materials, especially temperature-dependent semiconductor devices, require different thermal load analyses. The micromechanical structures of thermal, elastic and plasma field in Green and Naghdi theory has been previously analyzed by Todorovic et al. [2–4]. The theory developed by Lord and Shulman [5] uses a single relaxation time to compute the motion generated by a finitely fast thermal field. Marin et al. [6] studied the extensions of the domain of influences theory for generalized thermoelastic of anisotropic materials with voids. Ezzat and El-Bary [7] studied the effects of fractional derivatives and magnetic field in thermoelastic material under phase-lag GN models. Abbas [8] applied eigenvalue approaches to the fractional order model of thermo-diffusion problems for an unbounded elastic medium with spherical cavities. Abbas et al. [9] studied the propagations of waves in a generalized thermoelastic plane by an eigenvalue approach. Alharbi et al. [10] studied the influences of

initial stresses and varying thermal conductivity on fiber-reinforced magneto-thermoelastic media under microtemperatures. Shuangquan and Tianhu [11] presented a study on the transient responses of porous mediums with strain and thermal relaxations. Abouelregal and Tiwari [12] studied the effects of memory-dependent heat conduction on thermoelastic vibrations of a nano-sized rotating beam with varying thermal properties under axial load. Several authors [13–20] have proposed solutions to various problems by using the thermoelasticity theory. Ailawalia and Kumar [21] investigated how photothermal interactions manifest in semiconductor media due to ramp-type heating. Abbas et al. [22] looked at photothermal interactions in semiconductors using the DPL model. Heat transfer in convective fins of varying thermal conductivity and heating generation was studied by Ghasemi et al. [23]. Energy pile displacement under thermal and mechanical loading was the subject of a numerical study by Yang et al. [24]. Using photo-thermoelastic excitations, Lotfy et al. [25] discussed the Thomson and electromagnetic effects of laser pulses on semiconductor materials. The effects of ramp-type heating on photo-thermo-elastic waves in a semi-conductor have been investigated by Hobiny et al. [26]. Mohamed et al. [27] looked at the absorption illuminations of semi-infinite thermoelastic materials with a rotator in two dimensions using a modified GL model.

Most thermoelastic studies consider thermal conductivity independent of temperature, which is only the case for some situations. At higher temperatures, as common in pipes conveying hot flow, missiles, nuclear reactors, etc., material properties may not remain constant. In the view of variable thermal conductivity with Kirchhoff's transforms, Youssef et al. [28] looked at the temperature dependence of the thermal conductivity and elastic modulus of a material in an unbounded medium containing spherical cavities. In [29], Sherief and Hamza model a thermoelastic hollow cylinder with variable thermal conductivity. Khoukhi et al. [30] evaluated the impact of varying thermal conductivity inside wall-encased insulations. Zenkour and Abbas [31] used a finite element model to analyze the nonlinear thermal transient stress of a temperature-dependent hollow cylinder. Mahdy et al. [32] studied the influences of variable thermal conductivity on wave propagations for ramp-type heating semiconductors in magneto-rotator hydrostatic stress media during photo-excited micro temperature processes. Abbas et al. [33] investigated the photothermal interaction in semiconductor media with cylindrical holes and varying thermal conductivity. In addition, the authors [34–41] applied Kirchhoff's transforms to solve nonlinear problems as linear problems.

The purpose of this study is to investigate how variations in thermal conductivity influence the transmission of waves through semiconductors. The nonlinear issue was solved using the finite element approach (without the use of Kirchhoff's transform). The linear problem (with Kirchhoff's transform) was solved using the Laplace transform and the eigenvalues technique. All physical quantities have numerical outcomes that are graphically shown. The accuracy of the suggested technique is confirmed by comparing the numerical solution to previously obtained analytic solutions by others while neglecting the new parameters, and by exploring the behavior of the solutions.

2. Mathematical Model

For homogeneous and isotropic semiconductor materials, the basic formulations are as follows, assuming the absence of any external heat source and body force [42–44]:

$$\mu u_{i,jj} + (\lambda + \mu) u_{j,ij} - \gamma_n N_{,i} - \gamma_t T_{,i} = \rho \frac{\partial^2 u_i}{\partial t^2}. \tag{1}$$

$$\left(K T_{,j}\right)_{,j} + \frac{E_g}{\tau} N = \left(1 + \tau_o \frac{\partial}{\partial t}\right)\left(\rho c_e \frac{\partial T}{\partial t} + \gamma_t T_o \frac{\partial u_{j,j}}{\partial t}\right), \tag{2}$$

$$D_e N_{,jj} - \frac{N}{\tau} + \frac{k}{\tau} T = \frac{\partial N}{\partial t}. \tag{3}$$

$$\sigma_{ij} = \mu\left(u_{i,j} + u_{j,i}\right) + (\lambda u_{k,k} - \gamma_n N - \gamma_t T)\delta_{ij}, \tag{4}$$

where ρ is the density of material, $N = n - n_o$, n_o refer to the carrier concentration at equilibrium, $i, j, k = 1, 2, 3$, c_e points to the heat specific at constant strain, λ, μ are the Lame's constants, $\gamma_n = (3\lambda + 2\mu)d_n$, d_n is the coefficient of electronic deformation, $\gamma_t = (3\lambda + 2\mu)\alpha_t$, α_t refers to the coefficients of linear thermal expansion, T_o is the reference temperature, t refers to the time, D_e refers to the carrier diffusion coefficient, u_i refers to the components of displacement, σ_{ij} are the stresses components, $T = T^* - T_o$, T^* is the increment of temperature, $k = \frac{\partial n_o}{\partial T}$ is the coupling parameter of thermal activation [42], and τ is the photo-generated carrier lifetime. Considered to be temperature-dependent, K denotes thermal conductivity. We shall analyze the linear expression for the thermal conductivity as in [45]:

$$K(T) = K_o(1 + K_s T), \tag{5}$$

where K_o is the thermal conductivity when $T = T_o$ and $K_s \leq 0$ points to the non-positive parameter. Considering the case of infinite isotropic semiconductor mediums whose states may be represented as functions of the spatial variable x and the time variable t leads to the formulation of the Equations (1)–(4) by [29]:

$$(\lambda + 2\mu)\frac{\partial^2 u}{\partial x^2} - \gamma_t \frac{\partial T}{\partial x} - \gamma_n \frac{\partial N}{\partial x} = \rho \frac{\partial^2 u}{\partial t^2}, \tag{6}$$

$$K_o(1 + K_s T)\frac{\partial^2 T}{\partial x^2} + K_o K_s \left(\frac{\partial T}{\partial x}\right)^2 + \frac{E_g}{\tau} N = \left(1 + \tau_o \frac{\partial}{\partial t}\right)\left(\rho c_e \frac{\partial T}{\partial t} + \gamma_t T_o \frac{\partial^2 u}{\partial t \partial x}\right), \tag{7}$$

$$\frac{\partial N}{\partial t} = D_e \frac{\partial^2 N}{\partial x^2} + \frac{k}{\tau} T - \frac{N}{\tau}, \tag{8}$$

$$\sigma_{xx} = (\lambda + 2\mu)\frac{\partial u}{\partial x} - \gamma_t T - \gamma_n N. \tag{9}$$

3. Application

The starting condition should be homogenous, and the boundary conditions at $x = 0$ are given by

$$u(0, t) = 0, \tag{10}$$

$$T(0, t) = T_1 H(t), \tag{11}$$

$$D_e \left.\frac{\partial N(x, t)}{\partial x}\right|_{x=0} = s_1 N(0, t), \tag{12}$$

where T_1 is the constant temperature, s_1 is the surface recombination velocity and $H(t)$ is the Heaviside unit function. The non-dimensional parameters may be conveniently stated as:

$$(x', u') = \eta c(x, u),\ K_s' = T_o K_s, N' = \frac{N}{n_o}, T' = \frac{T}{T_o},\ \sigma_{xx}' = \frac{\sigma_{xx}}{\lambda + 2\mu}, (t', \tau', \tau_o') = \eta c^2(t, \tau, \tau_o), \tag{13}$$

where $\eta = \frac{\rho c_e}{K}$ and $c = \sqrt{\frac{\lambda + 2\mu}{\rho}}$.

Now, if we ignore the dashes, we may write out the governing equations in a non-dimensional form using parameters (13).

$$\frac{\partial^2 u}{\partial x^2} - a_1 \frac{\partial N}{\partial x} - a_2 \frac{\partial T}{\partial x} = \frac{\partial^2 u}{\partial t^2}, \tag{14}$$

$$\frac{\partial^2 N}{\partial x^2} - \frac{a_3}{\tau} N + \frac{\alpha}{\tau} T = a_3 \frac{\partial N}{\partial t}, \tag{15}$$

$$(1+K_sT)\frac{\partial^2 T}{\partial x^2}+K_s\left(\frac{\partial T}{\partial x}\right)^2+\frac{a_4}{\tau}N=\left(1+\tau_o\frac{\partial}{\partial t}\right)\left(\frac{\partial T}{\partial t}+a_5\frac{\partial^2 u}{\partial t\partial x}\right), \tag{16}$$

$$\sigma_{xx}=\frac{\partial u}{\partial x}-a_1N-a_2T, \tag{17}$$

$$u(0,t)=0,\ T(0,t)=T_1H(t),\ \left.\frac{\partial N(x,t)}{\partial x}\right|_{x=0}=a_6N(0,t), \tag{18}$$

where $a_1=\frac{\gamma_n n_o}{\lambda+2\mu}$, $a_2=\frac{\gamma_t T_o}{\lambda+2\mu}$, $a_3=\frac{1}{\eta D_e}$, $a_4=\frac{E_g n_o}{T_o\rho c_e}$, $a_5=\frac{\gamma_t}{\rho c_e}$, $a_6=\frac{s_1}{D_e\eta c}$ and $\alpha=\frac{T_o k}{n_o c^2 D_e\eta^2}$.

4. Numerical Solution (Finite Element Method)

In this section, we establish the fundamental forms of the equations, which are nonlinear partial differential equations. The potential solutions to this problem are investigated using the finite element technique (FEM). Similar to [46,47], this strategy employs the standard weak formulation techniques. The weak formulations of the essential equations are fixed in a non-dimensional setting. The sets of independent weight functions are presented, which include the carrier density N, temperature T, and displacement u. Integrating across the spatial domain involves multiplying the basic equations by the independent weight functions, as dictated by the problem's boundary conditions. So, we may express the carrier density, temperature, and displacement values at each node as follows:

$$T=\sum_{j=1}^{m}M_jT_j(t),\ N=\sum_{j=1}^{m}M_jN_j(t),\ u=\sum_{j=1}^{m}M_ju_j(t), \tag{19}$$

where m denotes the node's number of elements, and M refers to the shape functions, where the shape functions and weight function are identical to Galerkin's standard methods. Therefore,

$$\delta T=\sum_{j=1}^{m}M_j\delta T_j,\ \delta N=\sum_{j=1}^{m}M_j\delta N_j,\ \delta u=\sum_{j=1}^{m}M_j\delta u_j. \tag{20}$$

The implicit techniques should be used to derive the time derivatives of the unknown variables in the following phase. The weak formulations for FEM that correspond to (14)–(16) are now as follows:

$$\int_0^L\frac{\partial\delta u}{\partial x}\left(\frac{\partial u}{\partial x}-a_1N-a_2T\right)dx+\int_0^L\delta u\left(\frac{\partial^2 u}{\partial t^2}\right)dx=\delta u\left(\frac{\partial u}{\partial x}-a_1N-a_2T\right)_0^L, \tag{21}$$

$$\int_0^L\frac{\partial\delta N}{\partial x}\left(\frac{\partial N}{\partial x}\right)dx+\int_0^L\delta u\left(\frac{a_3}{\tau}N-\frac{\alpha}{\tau}T+a_3\frac{\partial N}{\partial t}\right)dx=\delta u\left(\frac{\partial N}{\partial x}\right)_0^L. \tag{22}$$

$$\int_0^L\frac{\partial\delta T}{\partial x}(1+K_sT)\frac{\partial T}{\partial x}dx+\int_0^L\delta T\left(-\frac{a_4}{\tau}N+\left(1+\tau_o\frac{\partial}{\partial t}\right)\left(\frac{\partial T}{\partial t}+a_5\frac{\partial^2 u}{\partial t\partial x}\right)\right)dx=\delta T\left((1+K_sT)\frac{\partial T}{\partial x}\right)_0^L, \tag{23}$$

5. Linear Cases (with Kirchhoff's Transforms)

In order to change the basic equations from a nonlinear form into a linear one, we use Kirchhoff's transforms mapping [45] to varying thermal conductivity, which is shown in the equation. This allows us to convert the essential forms (5)

$$\theta=\frac{1}{K_o}\int_0^T K(T)dT, \tag{24}$$

where the recently added function represents the conduction of heat. We may get [45] by substituting from Equation (24) in (5), then integrating.

$$\theta = T + \frac{1}{2}K_s T^2. \tag{25}$$

The following may be concluded from Equations (24) and (25):

$$K_o\theta_{,i} = K(T)T_{,i},\ K_o\theta_{,ii} = (K(T)T_{,i})_{,i},\ K_o\frac{\partial\theta}{\partial t} = K(T)\frac{\partial T}{\partial t}. \tag{26}$$

Consequently, the governing Equations (14)–(18), may be stated in the linear form:

$$\frac{\partial^2 u}{\partial x^2} - a_1\frac{\partial N}{\partial x} - a_2\frac{\partial\theta}{\partial x} = \frac{\partial^2 u}{\partial t^2}, \tag{27}$$

$$\frac{\partial^2 N}{\partial x^2} - \frac{a_3}{\tau}N + \frac{\alpha}{\tau}\theta = a_3\frac{\partial N}{\partial t}, \tag{28}$$

$$\frac{\partial^2\theta}{\partial x^2} + \frac{a_4}{\tau}N = (1+\tau_o\frac{\partial}{\partial t})(\frac{\partial\theta}{\partial t} + a_5\frac{\partial^2 u}{\partial t\partial x}), \tag{29}$$

$$\sigma_{xx} = \frac{\partial u}{\partial x} - a_1 N - \frac{a_2}{K_s}\left(-1+\sqrt{1+2K_s\theta}\right), \tag{30}$$

$$u(0,t) = 0,\ \theta(0,t) = T_1H(t) + \frac{1}{2}K_s(T_1H(t))^2,\ \left.\frac{\partial N(x,t)}{\partial x}\right|_{x=0} = a_6N(0,t), \tag{31}$$

6. Analytical Solution

For the $g(x,t)$ function, Laplace transforms were written as

$$\overline{g}(x,s) = L[g(x,t)] = \int_0^\infty g(x,t)e^{-st}dt, \tag{32}$$

where s is the Laplace transformation parameter. Thus, the essential equations may be rewritten in the following ways:

$$\frac{d^2\overline{u}}{dx^2} = s^2\overline{u} + a_1\frac{d\overline{N}}{dx} + x_2\frac{d\overline{\theta}}{dx}, \tag{33}$$

$$\frac{d^2\overline{N}}{dx^2} = a_3\left(s+\frac{1}{\tau}\right)\overline{N} - \frac{\beta}{\tau}\overline{\theta}, \tag{34}$$

$$\frac{d^2\overline{\theta}}{dx^2} = s(1+\tau_o s)\theta - \frac{a_4}{\tau}\overline{N} + a_5 s(1+\tau_o s)\frac{d\overline{u}}{dx}, \tag{35}$$

$$\overline{\sigma}_{xx} = \frac{d\overline{u}}{dx} - a_1\overline{N} - \frac{a_2}{K_s}\left(-1+\sqrt{1+2K_s\overline{\theta}}\right), \tag{36}$$

$$\overline{u}(0,t) = 0,\ \left.\frac{d\overline{N}(x,t)}{dx}\right|_{x=0} = x_6\overline{N}(0,t),\ \overline{\theta}(0,t) = \frac{T_1}{s}\left(1+\frac{1}{2s}T_1K_s\right), \tag{37}$$

Now, using the eigenvalue approach provided in [48–50], we will get the solutions of the coupled differential system (33)–(35) with the boundary conditions (37). We may get the matrices and vectors from Equations (33)–(35) as

$$\frac{d\mathrm{V}}{dx} = AV, \tag{38}$$

where $V = \left[\overline{u} \quad \overline{N} \quad \overline{\phi} \quad \frac{d\overline{u}}{dx} \quad \frac{d\overline{N}}{dx} \quad \frac{d\overline{\phi}}{dx}\right]^T$ and $A = \left[a_{ij}\right]_{6\times 6}$ with $a_{ij} = 0$, expect $a_{14} = 1$, $a_{25} = 1$, $a_{36} = 1$, $a_{41} = s^2$, $a_{45} = a_1$, $a_{46} = a_2$, $a_{52} = a_3\left(s + \frac{1}{\tau}\right)$, $a_{53} = -\frac{\beta}{\tau}$, $a_{62} = -\frac{a_4}{\tau}$, $a_{63} = s(1 + \tau_o s)$, $a_{64} = s(1 + \tau_o s)a_5$.

The equations that characterize matrix A are given

$$\omega^6 - b_1\omega^4 + b_2\omega^2 + b_3 = 0, \tag{39}$$

where $b_1 = a_{52} + a_{63} + a_{41} + a_{46}a_{64}$, $b_3 = a_{41}a_{62}a_{53} - a_{63}a_{41}a_{52}$, $b_2 = -a_{64}a_{45}a_{53} + a_{41}a_{63} + a_{64}a_{46}a_{52} + a_{52}a_{41} + a_{63}a_{52} - a_{53}a_{62}$. The six roots of Equation (40) are the six eigenvalues of matrix A, which are written as $\pm\omega_1$, $\pm\omega_2$ and $\pm\omega_3$. Thus, the eigenvectors Y are computed as: $Y_1 = \left(a_{52} - \omega^2\right)a_{46}\omega - a_{45}a_{53}\omega$, $Y_2 = a_{53}\left(a_{41} - \omega^2\right)$, $Y_3 = \left(a_{52} - \omega^2\right)\left(\omega^2 - a_{41}\right)$, $Y_4 = \omega Y_1$, $Y_5 = \omega Y_2$, $Y_6 = \omega Y_3$.

The solutions of Equation (40) have the following form:

$$\mathrm{V}(x, s) = \sum_{i=1}^{3}\left(A_i Y_i e^{-\omega_i x} + A_{i+1}Y_{i+1}e^{\omega_i x}\right) \tag{40}$$

The rising exponential nature of the variable x has been removed to infinity due to the regularity constraint of the solution. Hence, the general solutions (40) may be shown as

$$\mathrm{V}(x, s) = \sum_{i=1}^{3} A_i Y_i e^{-\omega_i x} \tag{41}$$

where A_1, A_2 and A_3 are constants which can be calculated through the use of the problem's boundary conditions. To get the final solutions of displacement, temperature, carrier density, and stresses distributions, the Fourier series approximation [51] may be employed as a numerical inversion approach.

7. Discussion of Numerical Results

The results are theoretically investigated using the physical constants and physical characteristics of silicon as an elastic semiconductor material. Calculations and explanations of results from numerical simulations are made possible using constants derived from silicon (Si). The constants of Si are [52]:

$$\lambda = 3.64 \times 10^{10}\frac{N}{m^2}, E_g = 1.11\ eV,\ \mu = 5.46 \times \frac{10^{10}N}{m^2}, T_o = 300\ \mathrm{k}, T_s = 1,$$

$$c_e = 695\ J/kgk, d_n = -9 \times 10^{-31}m^3,\ \alpha_t = 3 \times 10^{-6}k^{-1}, \tau = 5 \times 10^{-5}s,$$

$$s_f = 2\frac{\mathrm{m}}{\mathrm{s}},\ \rho = 2330\ \mathrm{kg}/m^3, n_o = 10^{20}m^{-3}, D_e = 2.5 \times 10^{-3}m^3/s.$$

Using these values, we can do numerical simulations of the physical variables over the distance x to evaluate the effect of varying thermal conductivity within the context of the coupled photothermal theory with one relaxation time (see Figures 1–16). The field distributions, such as carrier density distributions (plasma waves), stress distributions (mechanical wave distributions), displacement distributions (strain wave distributions), and thermal wave distributions (thermal temperature distribution), are used in the numerical calculations. For the time $t = 0.8$, a numerical calculation is performed. Figure 1 predicts the increment of temperature along the distance x. For the generalized photo-thermal theory, it has been observed that the temperature begins at its maximum value, according to the applied boundary condition, then decreases with increasing x. It then decreases gradually as the distance x increases until it approaches zero beyond a wavefront.

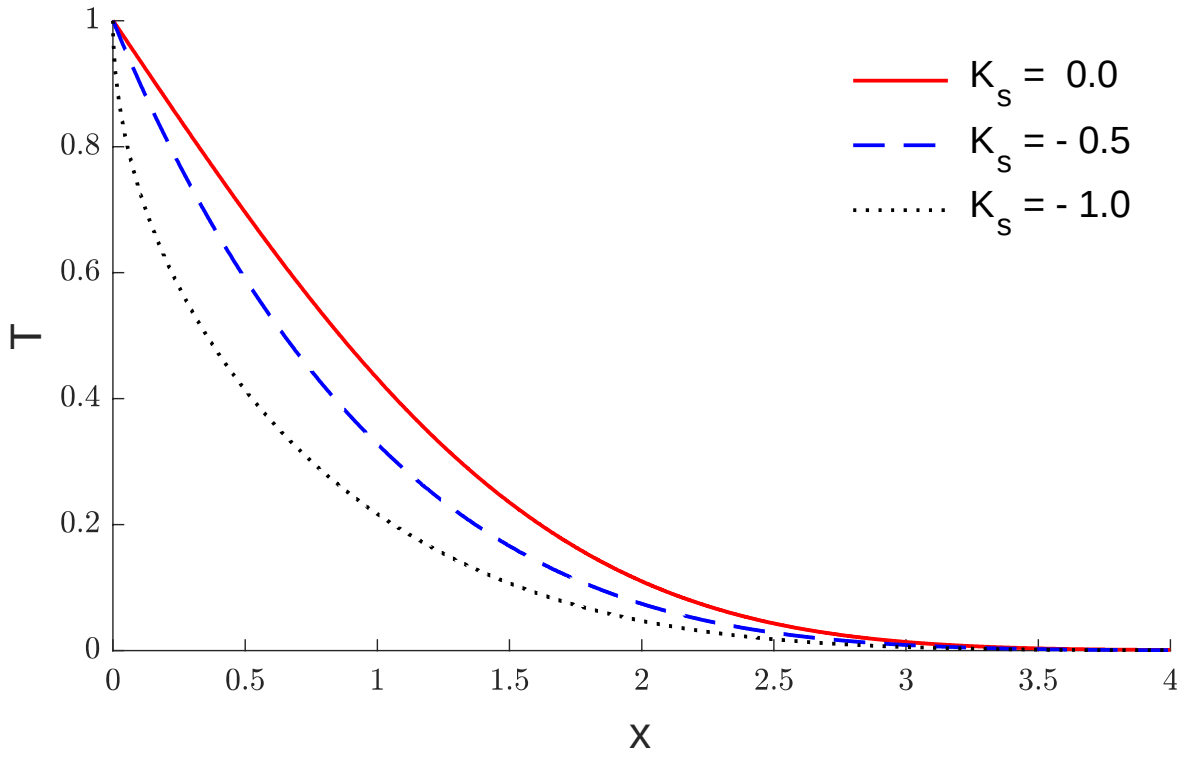

Figure 1. The variation of temperature under various values of K_s.

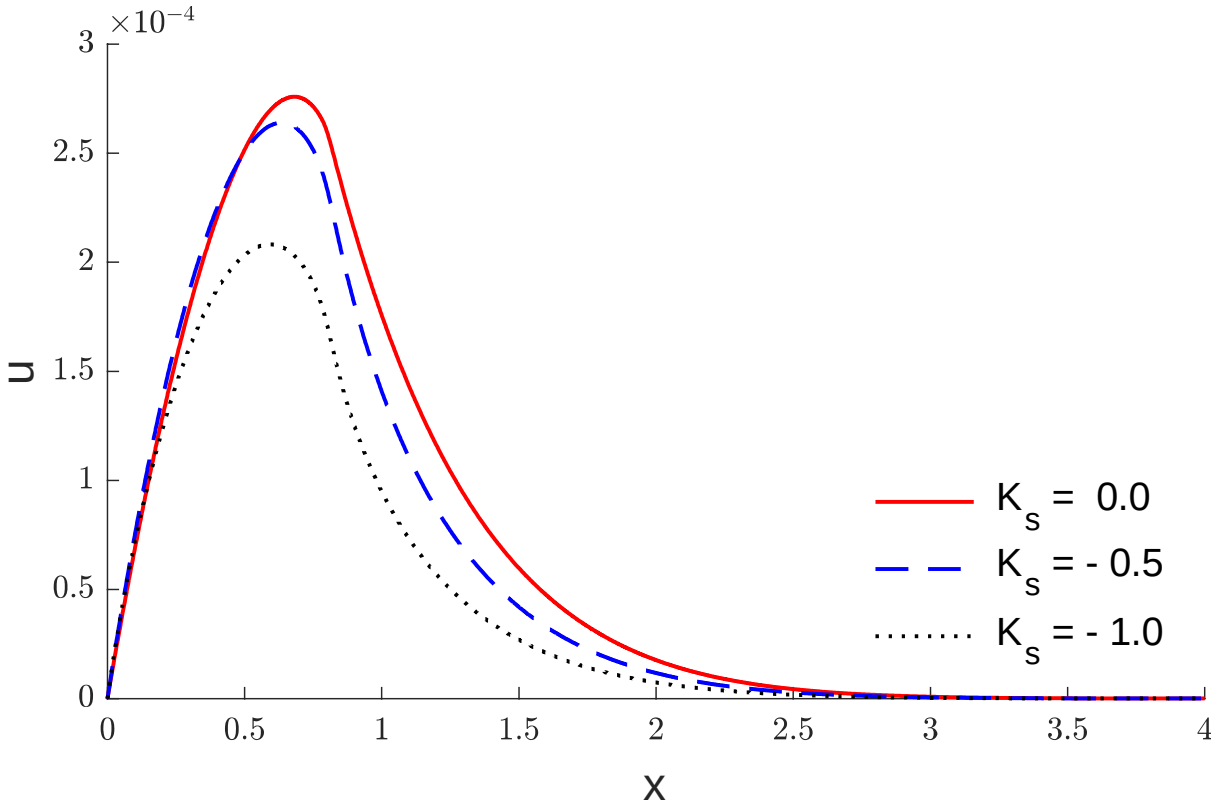

Figure 2. The displacement variations under various values of K_s.

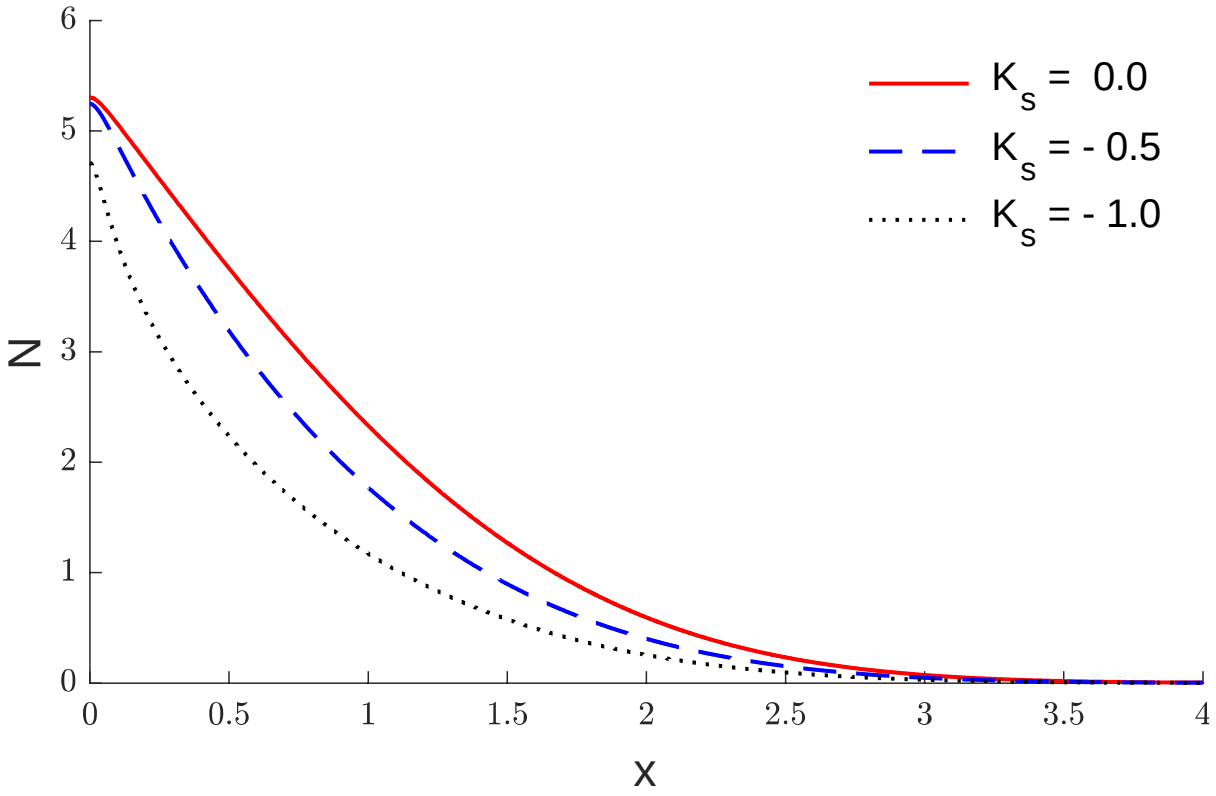

Figure 3. The carrier density variations under various values of K_s.

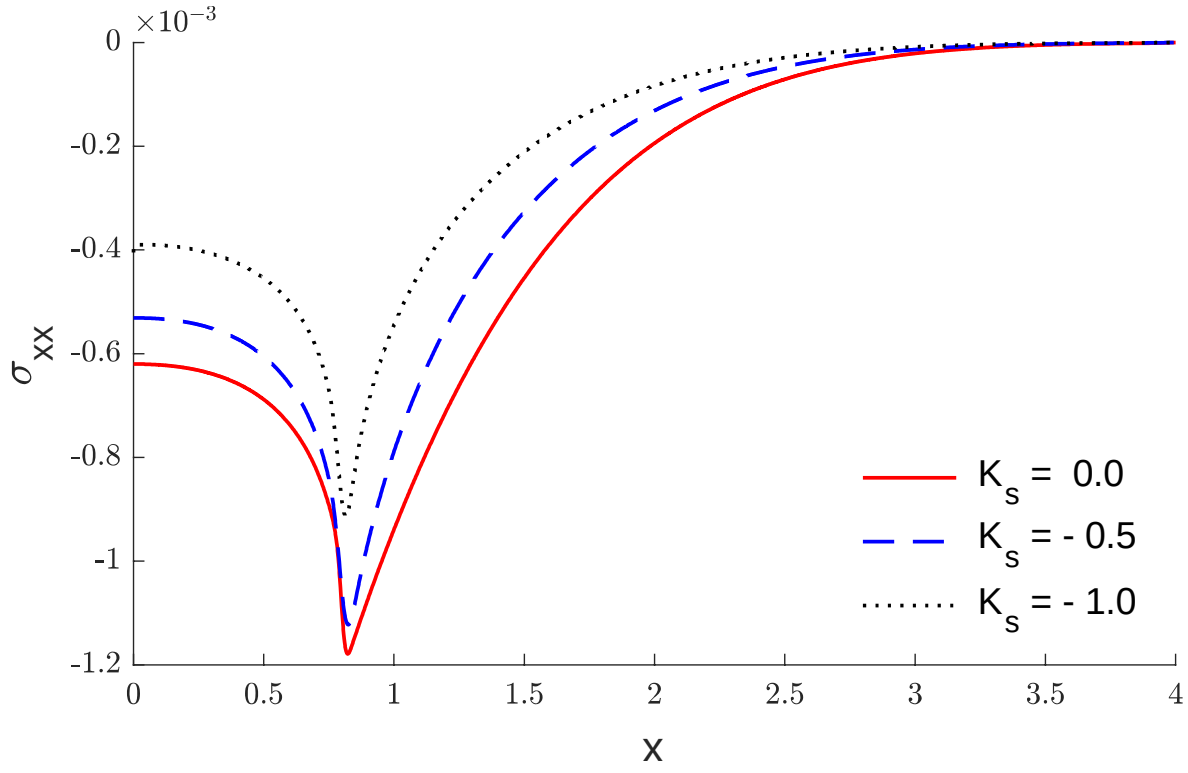

Figure 4. The stress variations under various values of K_s.

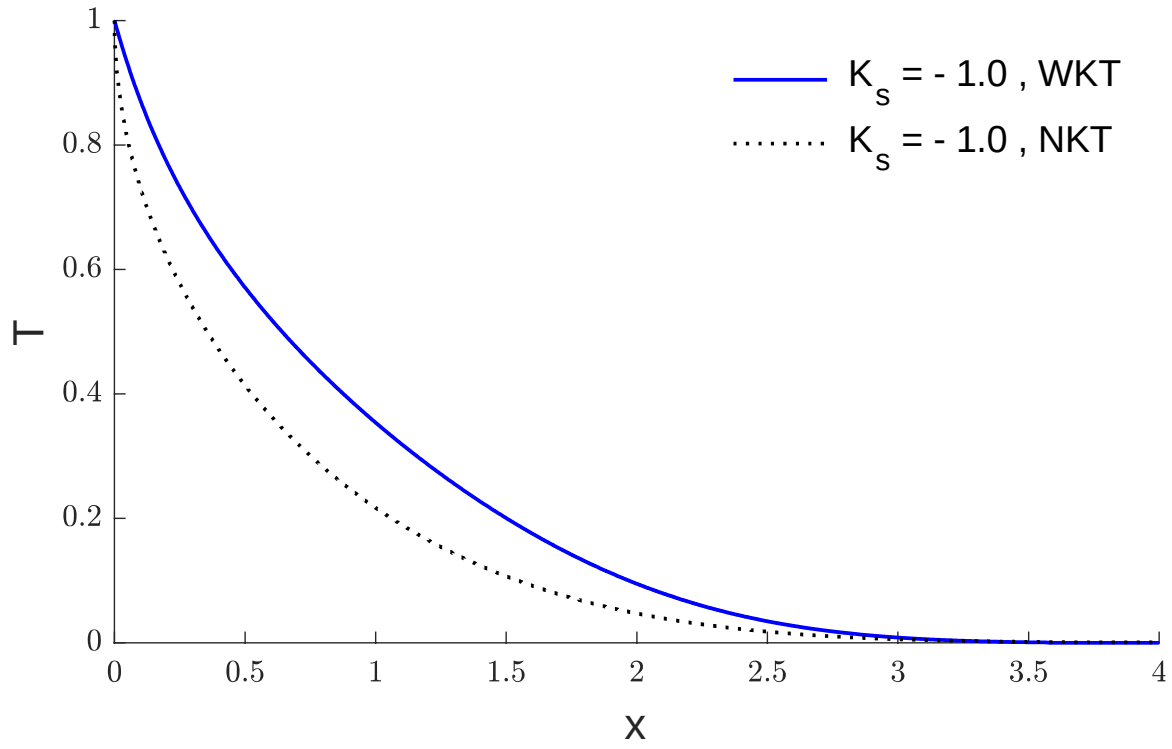

Figure 5. The variations of temperature with and without Kirchhoff transforms when $K_s = -1$.

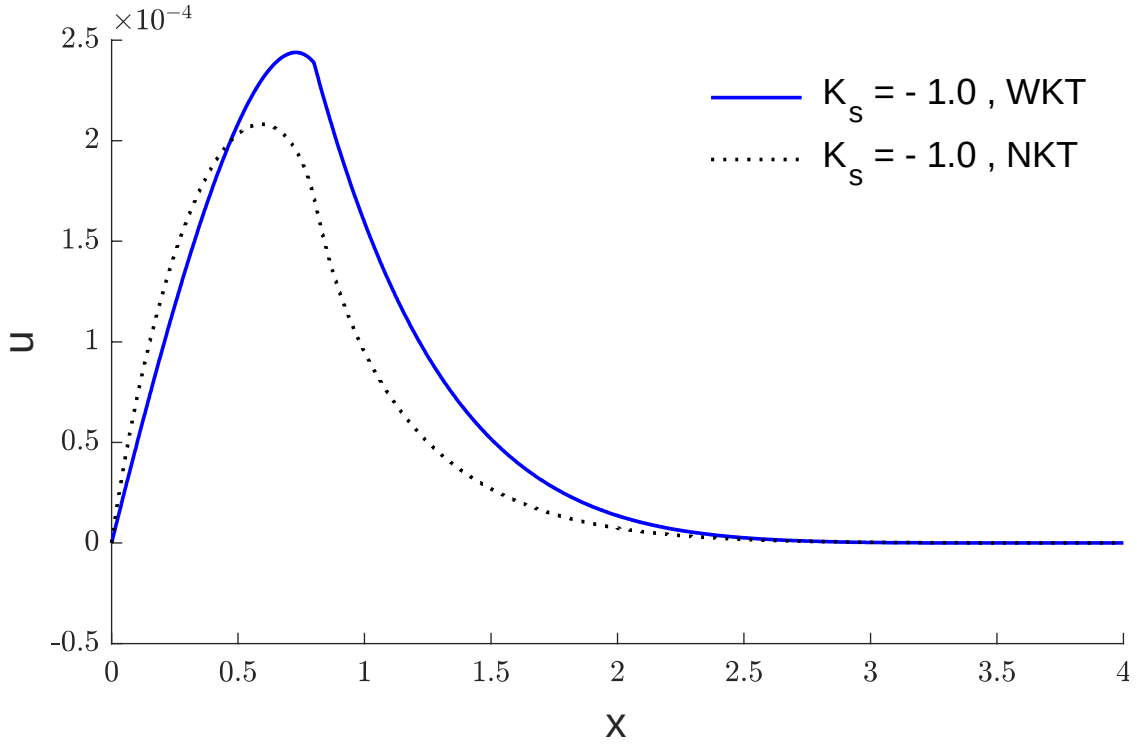

Figure 6. The variations of displacement with and without Kirchhoff transforms when $K_s = -1$.

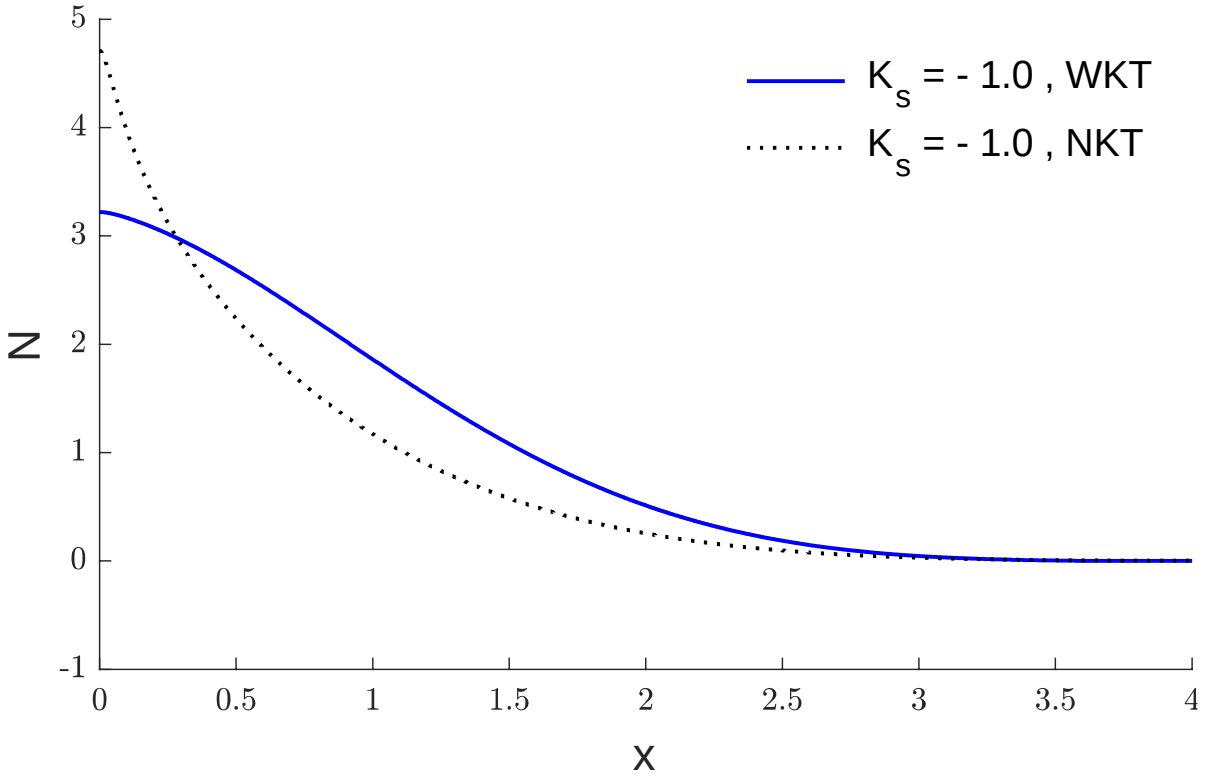

Figure 7. The variations of carrier density with and without Kirchhoff transforms when $K_s = -1$.

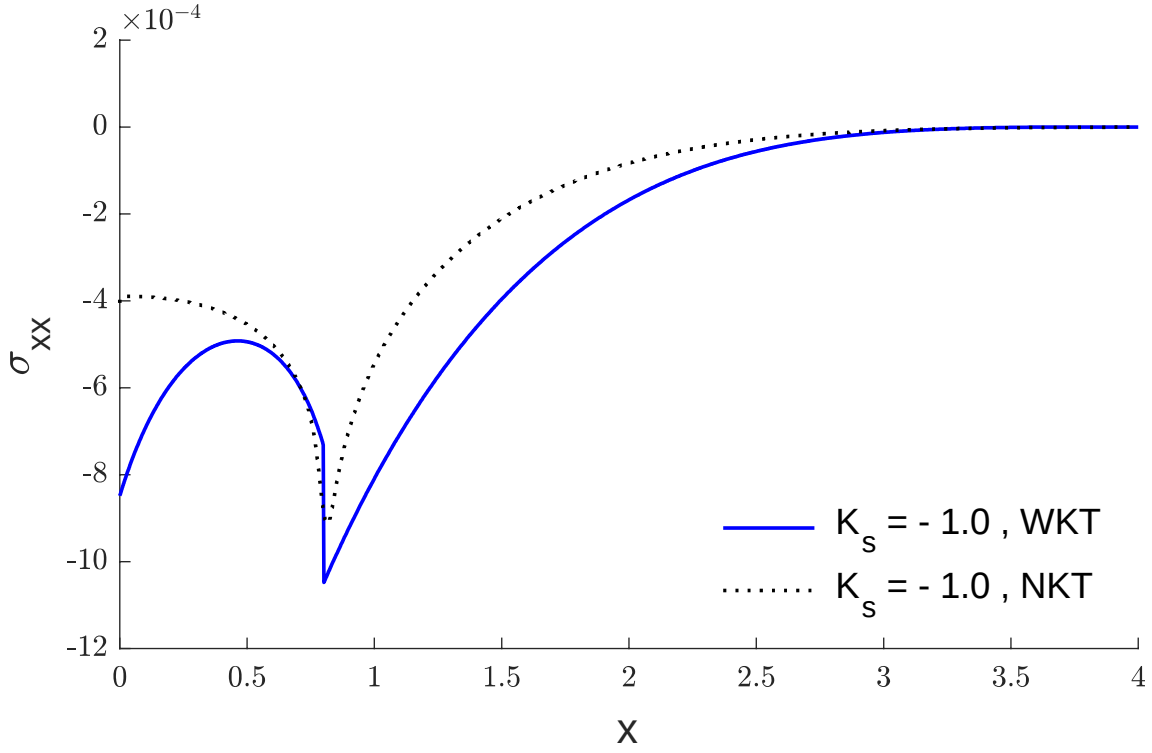

Figure 8. The variations of stress with and without Kirchhoff transforms when $K_s = -1$.

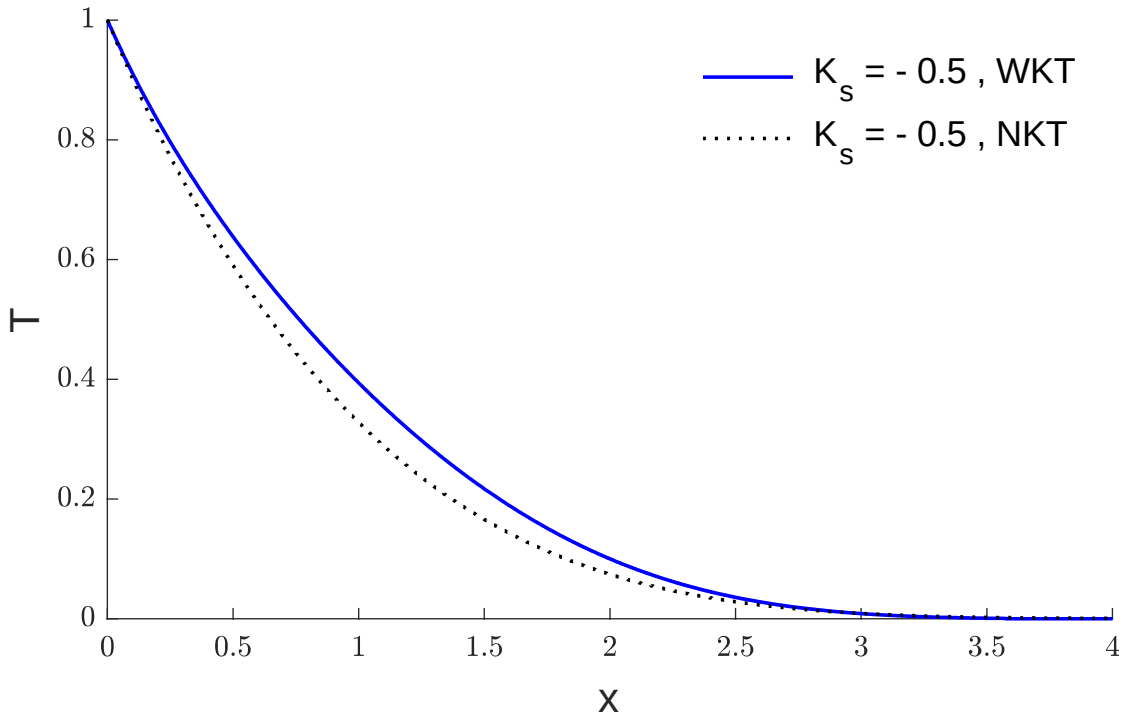

Figure 9. The variations of temperature with and without Kirchhoff transforms when $K_s = -0.5$.

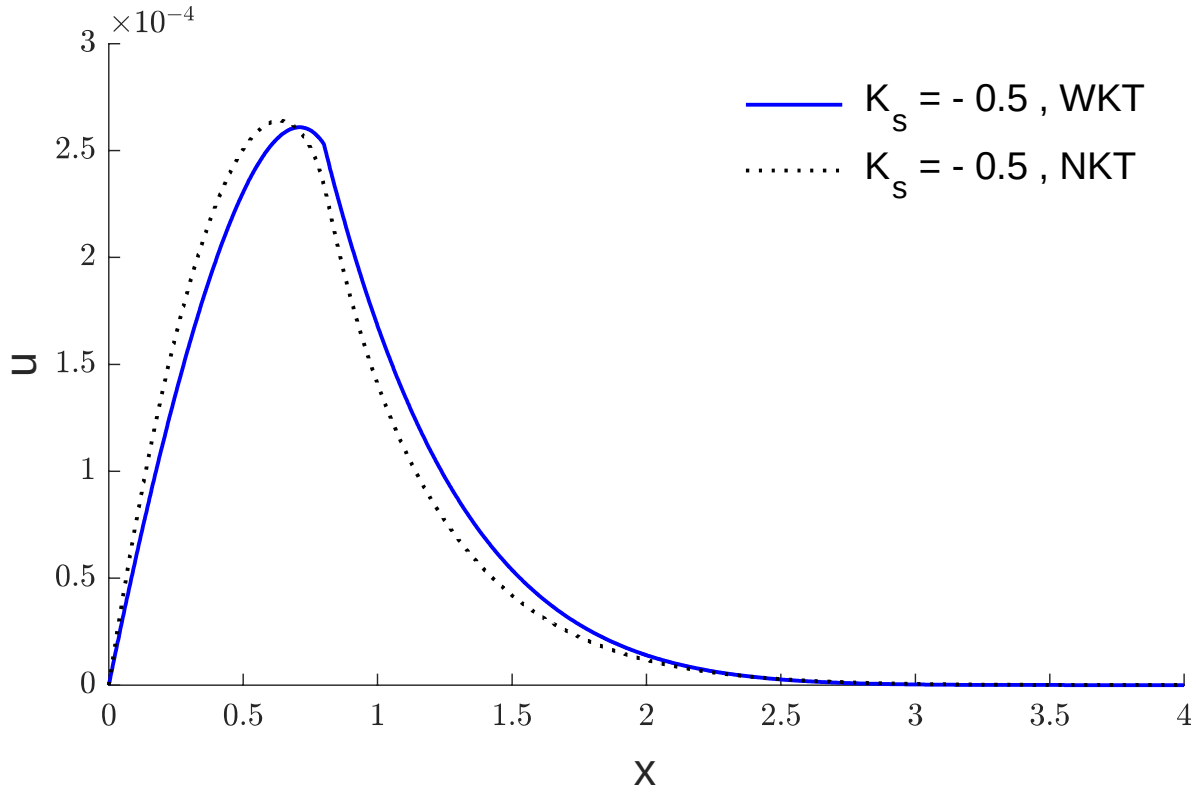

Figure 10. The variations of displacement with and without Kirchhoff transforms when $K_s = -0.5$.

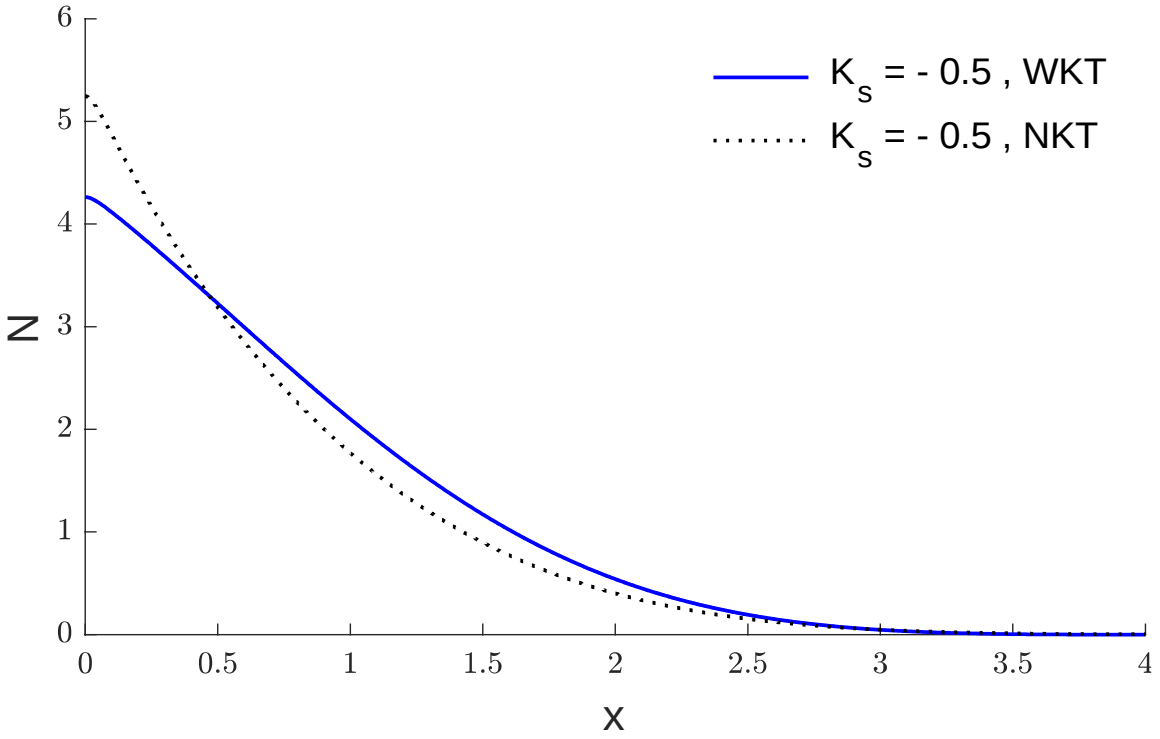

Figure 11. The variations of carrier density with and without Kirchhoff transforms when $K_s = -0.5$.

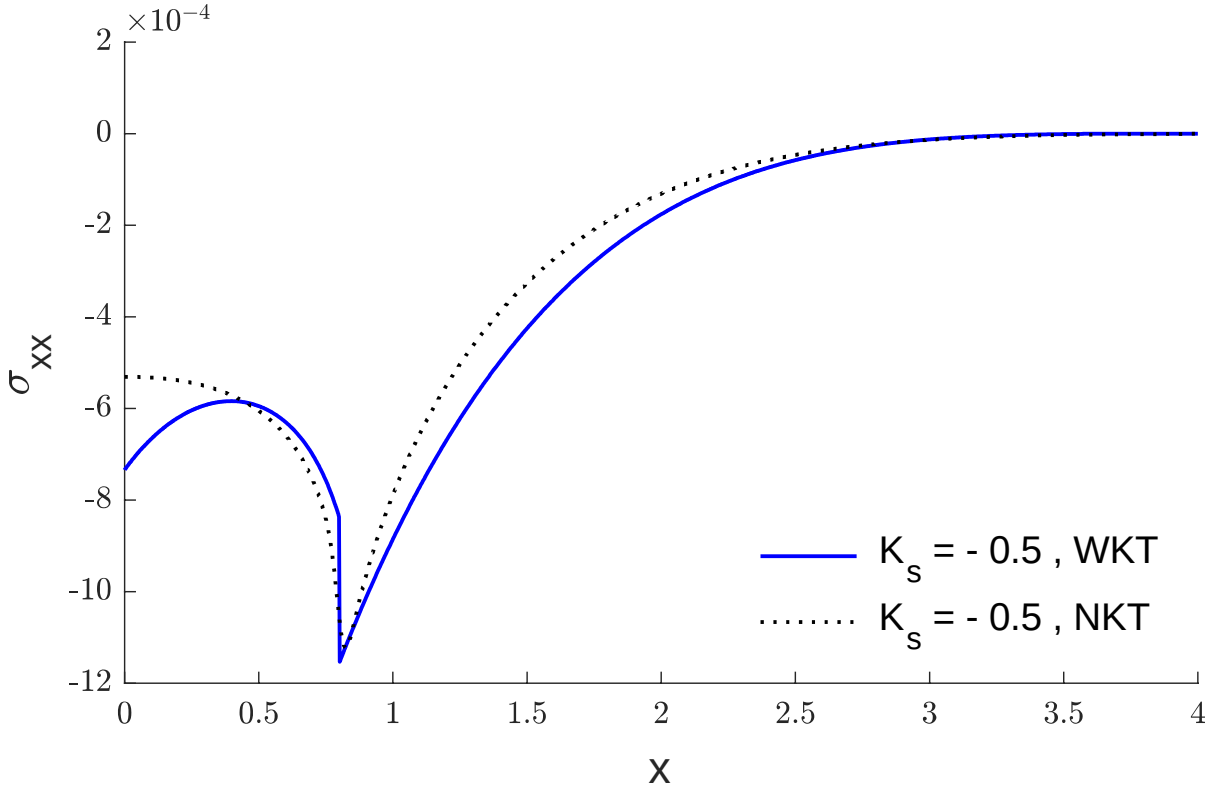

Figure 12. The stress variations with and without Kirchhoff transforms when $K_s = -0.5$.

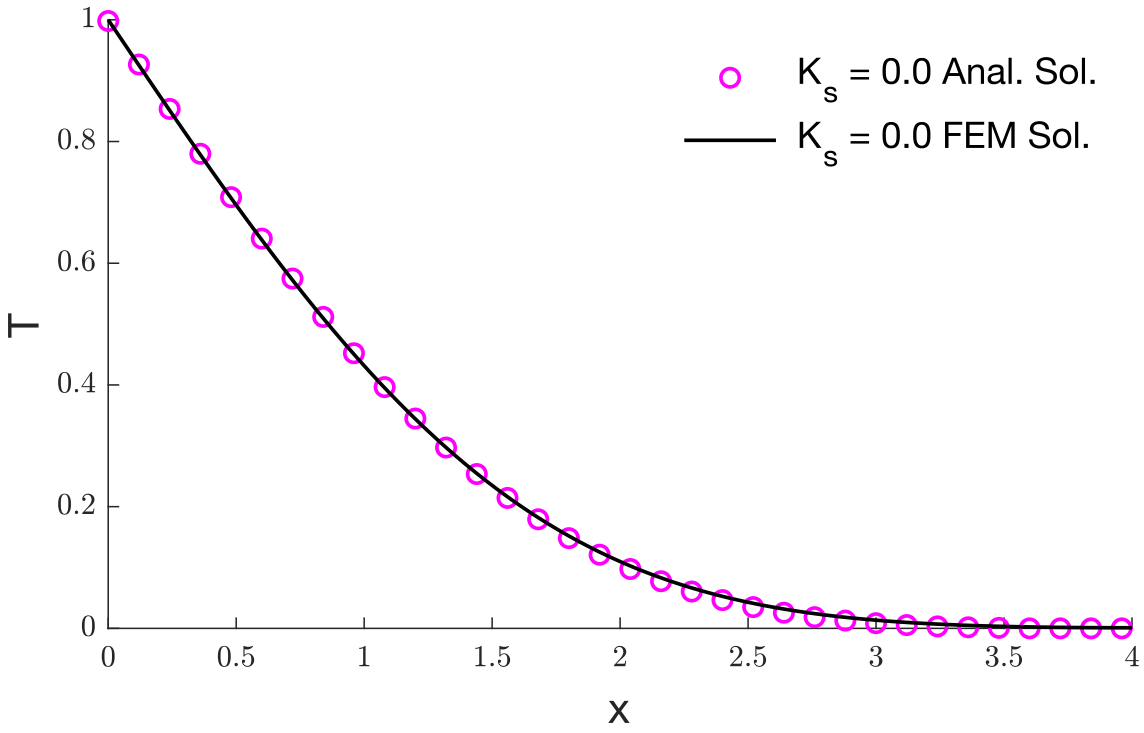

Figure 13. The study on temperature comparison.

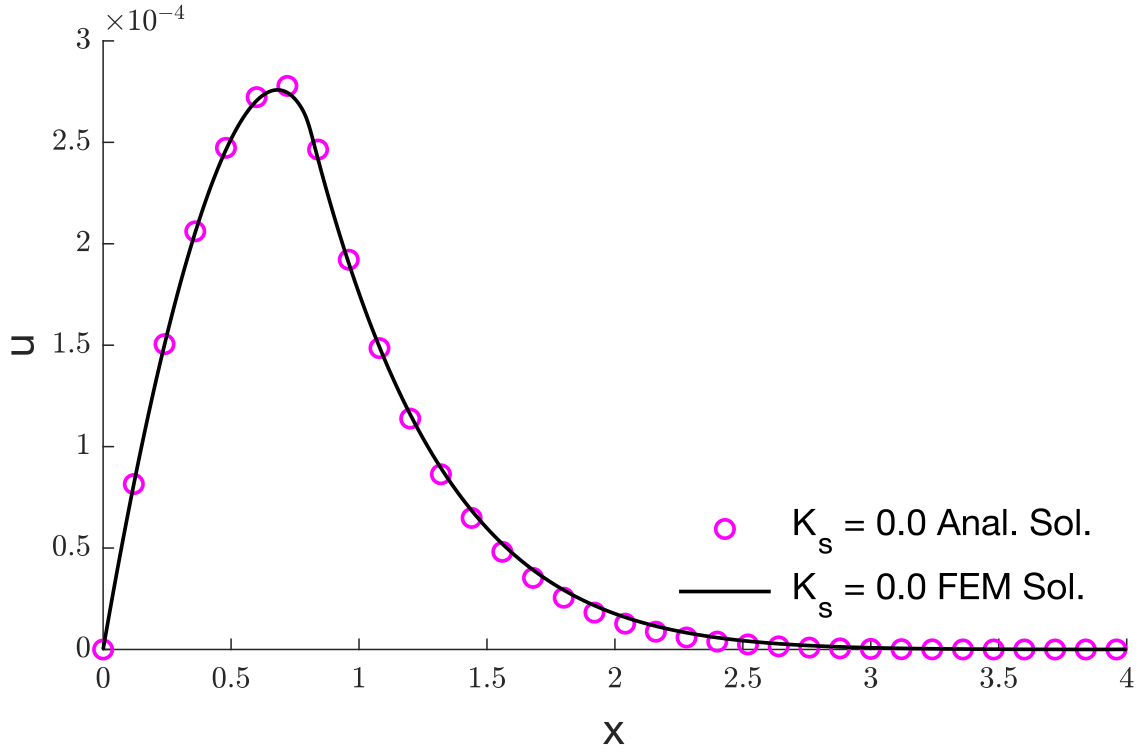

Figure 14. The study on displacement comparison.

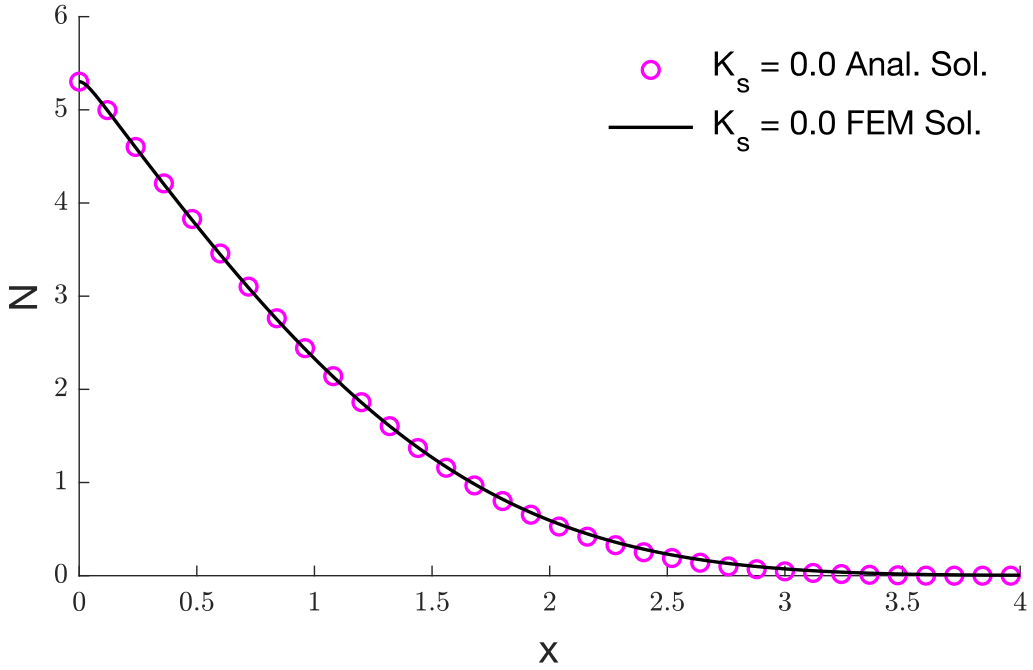

Figure 15. The study on carrier density comparison.

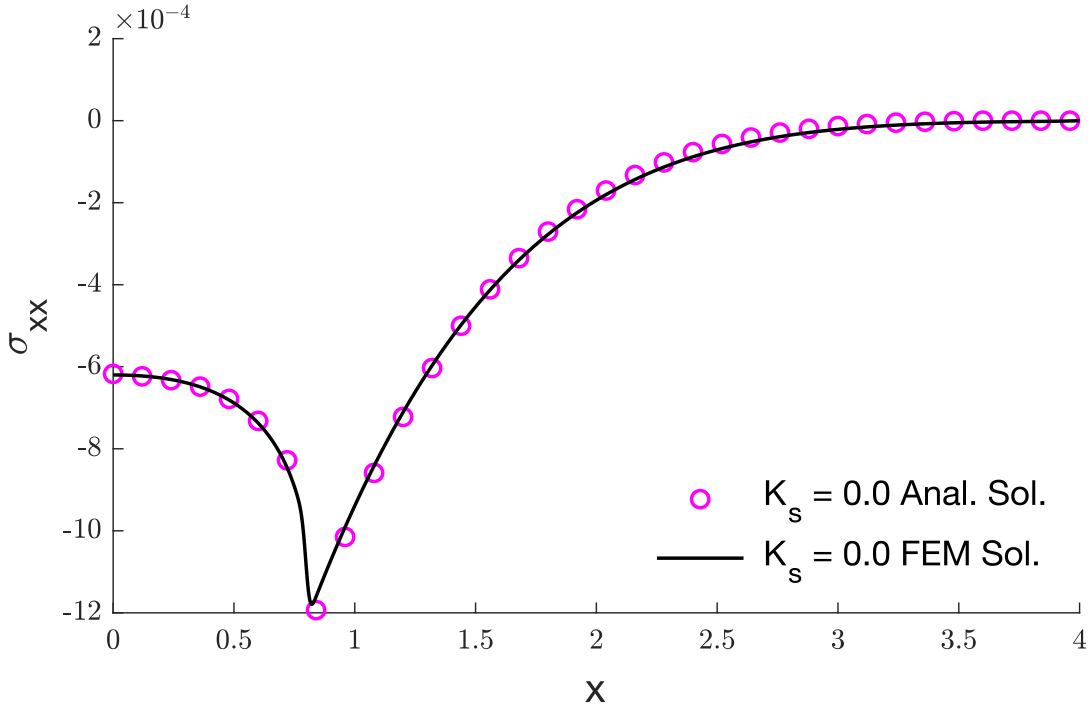

Figure 16. The study on stress comparison.

Figure 2 shows how the displacement changes with respect to the distance x. It was observed that the displacement of the zero values, according to the applied boundary condition, then rises with rising x, reaches a peak at a certain point relatively near to the surface, and then gradually falls to zero. Different carrier densities are shown as a function of x distance in Figure 3. At $x = 0$, where the surface is located, the carrier density is at its highest. As x increases, the carrier density slowly decreases until it is close to zero.

Figure 4 shows how the stress changes as x gets farther away. It is clear that the stress reaches some negative values, then slowly goes up until it reaches a peak of negative values,

and then slowly goes back down to zero. A comparison of the Kirchhoff transforms (WKT) and non-Kirchhoff transforms (NKT) results are shown in Figures 5–16. When $K_s = -1$, temperature, displacement, carrier density, and stress are all shown to vary along x. The usage of the Kirchhoff transforms (WKT) is shown by the solid line, whereas the absence of the transforms in the nonlinear situation is denoted by the dotted line (NKT). Figure 4 shows that the curves coincide at the surface since the temperature boundary condition is $T_1 = 1$. After that, the difference ratio grows with distance until x = 0.74, before falling to zero at x = 2.55. Figures 5–16 show the difference between using the Kirchhoff transforms (WKT) and not using the Kirchhoff transforms (NKT).

Figures 5–8 display how the temperature, displacement, carrier density, and stress change with respect to the distance x when $K_s = -1$. The solid line depicts the case when Kirchhoff transforms (WKT) are used, while the dotted line show the case when Kirchhoff transforms are not used (NKT). As shown in Figure 5, the curves are the same at the surface because the temperature boundary condition is $T_1 = 1$. After that, the difference ratio goes up as the distance goes up until $x = 1$, and then it goes down until it reaches zero at $x = 3.15$. Figure 6 depicts the displacement variation with and without Kirchhoff transforms. The curves coincide at the surface under the displacement boundary condition $(u = 0)$, where the difference ratio grows with distance until $x = 1$, and then reduces to zero at $x = 2.5$.

Figure 7 shows the carrier density variation with Kirchhoff transforms (WKT) and without Kirchhoff transforms (NKT), in which the curves have the ratio of a maximum difference on the surface $x = 0$. Figure 8 shows the variations of stress with Kirchhoff transforms (WKT) and without Kirchhoff transforms (NKT), where on the surface $x = 0$, the curves have the greatest difference ratio. When $K_s = -0.5$, the changes in temperature, displacement, carrier density, and stress along x are shown in Figures 9–12. It was discovered that, when comparing results obtained with and without Kirchhoff transforms (WKT), the differences are striking (NKT).

When $K_s = 0$, the analytical solutions (Laplace transforms and eigenvalue method with Kirchhoff transforms) are shown to be superior to the numerical solutions (finite element method without Kirchhoff transforms) in Figures 13–16. The analytical data strongly agree with the numerical results of temperature change, displacement variation, carrier density variation, and stress variation over x. As expected, the variable thermal conductivity parameter has significant effects on the speed of the wave propagation of all studied fields.

8. Conclusions

In this paper, the mathematical implications of changing thermal conductivity in semiconductor media with and without Kirchhoff's transformations are investigated. Without using Kirchhoff's transformations, the finite element approach yields numerical solutions for nonlinear equations. For nonlinear equations using Kirchhoff's transformations, the eigenvalue approach is used to provide an analytical solution. It was determined that the variable thermal conductivity has a considerable effect on the deformation behaviors of various physical field components. The numerical results and findings reported in this study should be helpful for scholars working on the advancement of solid mechanics as well as those in scientific and technical domains. Numerous thermodynamics problems may be solved by using the approaches presented in this article. The theoretical conclusions presented here can be of interest for experimental scientists and researchers working on this topic.

Author Contributions: Formal analysis, I.A.; Funding acquisition, A.H.; Investigation, A.H.; Methodology, I.A.; Visualization, I.A. All authors have read and agreed to the published version of the manuscript.

Funding: This research work was funded by Institutional Fund Projects under grant no. (IFPIP: 7-130-1443). The authors gratefully acknowledge technical and financial support provided by the Ministry of Education and King Abdulaziz University, DSR, Jeddah, Saudi Arabia.

Data Availability Statement: Not applicable.

Conflicts of Interest: The authors declare no conflict of interest.

References

1. He, C.F.; Lu, G.G.; Shan, X.N.; Sun, Y.F.; Li, T.; Qin, L.; Yan, C.L.; Ning, Y.Q.; Wang, L.J. Theoretical analysis of 980 nm high power Vertical External-cavity Surface-emitting Semiconductor Laser (VECSEL). In Proceedings of the ICO20: Optical Devices and Instruments, Changchun, China, 21–26 August 2005; pp. 204–213.
2. Todorović, D.M. Plasma, thermal, and elastic waves in semiconductors. *Rev. Sci. Instrum.* **2003**, *74*, 582–585. [CrossRef]
3. Todorović, D.M. Photothermal and electronic elastic effects in microelectromechanical structures. *Rev. Sci. Instrum.* **2003**, *74*, 578–581. [CrossRef]
4. Song, Y.; Cretin, B.; Todorovic, D.M.; Vairac, P. Study of photothermal vibrations of semiconductor cantilevers near the resonant frequency. *J. Phys. D Appl. Phys.* **2008**, *41*, 15516. [CrossRef]
5. Lord, H.W.; Shulman, Y. A generalized dynamical theory of thermoelasticity. *J. Mech. Phys. Solids* **1967**, *15*, 299–309. [CrossRef]
6. Marin, M.; Othman, M.I.A.; Abbas, I.A. An Extension of the Domain of Influence Theorem for Generalized Thermoelasticity of Anisotropic Material with Voids. *J. Comput. Theor. Nanosci.* **2015**, *12*, 1594–1598. [CrossRef]
7. Ezzat, M.A.; El-Bary, A.A. Fractional magneto-thermoelastic materials with phase-lag Green-Naghdi theories. *Steel Compos. Struct.* **2017**, *24*, 297–307. [CrossRef]
8. Abbas, I.A. Eigenvalue approach on fractional order theory of thermoelastic diffusion problem for an infinite elastic medium with a spherical cavity. *Appl. Math. Model.* **2015**, *39*, 6196–6206. [CrossRef]
9. Abbas, I.A.; Abdalla, A.E.N.N.; Alzahrani, F.S.; Spagnuolo, M. Wave propagation in a generalized thermoelastic plate using eigenvalue approach. *J. Therm. Stress.* **2016**, *39*, 1367–1377. [CrossRef]
10. Alharbi, A.M.; Said, S.M.; Abd-Elaziz, E.M.; Othman, M.I.A. Influence of Initial Stress and Variable Thermal Conductivity on a Fiber-Reinforced Magneto-Thermoelastic Solid with Micro-Temperatures by Multi-Phase-Lags Model. *Int. J. Struct. Stab. Dyn.* **2022**, *22*, 2250007. [CrossRef]
11. Li, Y.; He, T. Investigation of a half-space heated by laser pulses based on the generalized thermoelastic theory with variable thermal material properties. *Waves Random Complex Media* **2022**, *32*, 120–136. [CrossRef]
12. Abouelregal, A.E.; Tiwari, R. The thermoelastic vibration of nano-sized rotating beams with variable thermal properties under axial load via memory-dependent heat conduction. *Meccanica* **2022**, *57*, 2001–2025. [CrossRef]
13. Li, C.L.; Tian, X.G.; He, T.H. Analytical study of transient thermo-mechanical responses in a fractional order generalized thermoelastic diffusion spherical shell with variable thermal conductivity and diffusivity. *Waves Random Complex Media* **2021**, *31*, 1083–1106. [CrossRef]
14. Othman, M.I.A.; Zidan, M.E.M.; Mohamed, I.E.A. Dual-phase-lag model on thermo-microstretch elastic solid Under the effect of initial stress and temperature-dependent. *Steel Compos. Struct.* **2021**, *38*, 355–363. [CrossRef]
15. Zhang, L.; Bhatti, M.M.; Michaelides, E.E.; Marin, M.; Ellahi, R. Hybrid nanofluid flow towards an elastic surface with tantalum and nickel nanoparticles, under the influence of an induced magnetic field. *Eur. Phys. J. Spec. Top.* **2021**, *231*, 521–533. [CrossRef]
16. Scutaru, M.L.; Vlase, S.; Marin, M.; Modrea, A. New analytical method based on dynamic response of planar mechanical elastic systems. *Bound. Value Probl.* **2020**, *2020*, 104. [CrossRef]
17. Abouelregal, A.E.; Marin, M. The response of nanobeams with temperature-dependent properties using state-space method via modified couple stress theory. *Symmetry* **2020**, *12*, 1276. [CrossRef]
18. Hobiny, A.; Abbas, I.A. A study on the thermoelastic interaction in two-dimension orthotropic materials under the fractional derivative model. *Alex. Eng. J.* **2022**, *in press*. [CrossRef]
19. Alzahrani, F.; Hobiny, A.; Abbas, I.; Marin, M. An eigenvalues approach for a two-dimensional porous medium based upon weak, normal and strong thermal conductivities. *Symmetry* **2020**, *12*, 848. [CrossRef]
20. Abouelregal, A.E.; Marin, M. The Size-Dependent Thermoelastic Vibrations of Nanobeams Subjected to Harmonic Excitation and Rectified Sine Wave Heating. *Mathematics* **2020**, *8*, 1128. [CrossRef]
21. Ailawalia, P.; Kumar, A. Ramp Type Heating in a Semiconductor Medium under Photothermal Theory. *Silicon* **2019**, *12*, 347–356. [CrossRef]
22. Abbas, I.A.; Alzahrani, F.S.; Elaiw, A. A DPL model of photothermal interaction in a semiconductor material. *Waves Random Complex Media* **2018**, *29*, 328–343. [CrossRef]
23. Ghasemi, S.E.; Hatami, M.; Ganji, D.D. Thermal analysis of convective fin with temperature-dependent thermal conductivity and heat generation. *Case Stud. Therm. Eng.* **2014**, *4*, 1–8. [CrossRef]
24. Yang, W.; Zhang, L.; Zhang, H.; Wang, F.; Li, X. Numerical investigations of the effects of different factors on the displacement of energy pile under the thermo-mechanical loads. *Case Stud. Therm. Eng.* **2020**, *21*, 100711. [CrossRef]
25. Lotfy, K.; Hassan, W.; El-Bary, A.A.; Kadry, M.A. Response of electromagnetic and Thomson effect of semiconductor medium due to laser pulses and thermal memories during photothermal excitation. *Results Phys.* **2020**, *16*, 102877. [CrossRef]

26. Hobiny, A.D.; Alzahrani, F.S.; Abbas, I.A. A study on photo-thermo-elastic wave in a semi-conductor material caused by ramp-type heating. *Alex. Eng. J.* **2021**, *60*, 2033–2040. [CrossRef]
27. Mohamed, M.S.; Lotfy, K.; El-Bary, A.; Mahdy, A.M.S. Absorption illumination of a 2D rotator semi-infinite thermoelastic medium using a modified Green and Lindsay model. *Case Stud. Therm. Eng.* **2021**, *26*, 101165. [CrossRef]
28. Youssef, H.M.; Abbas, I.A. Thermal shock problem of generalized thermoelasticity for an infinitely long annular cylinder with variable thermal conductivity. *Comput. Methods Sci. Technol.* **2007**, *13*, 95–100. [CrossRef]
29. Sherief, H.H.; Hamza, F.A. Modeling of variable thermal conductivity in a generalized thermoelastic infinitely long hollow cylinder. *Meccanica* **2015**, *51*, 551–558. [CrossRef]
30. Khoukhi, M.; Abdelbaqi, S.; Hassan, A. Transient temperature change within a wall embedded insulation with variable thermal conductivity. *Case Stud. Therm. Eng.* **2020**, *20*, 100645. [CrossRef]
31. Zenkour, A.M.; Abbas, I.A. Nonlinear Transient Thermal Stress Analysis of Temperature-Dependent Hollow Cylinders Using a Finite Element Model. *Int. J. Struct. Stab. Dyn.* **2014**, *14*, 1450025. [CrossRef]
32. Mahdy, A.M.S.; Lotfy, K.; El-Bary, A.; Atef, H.M.; Allan, M. Influence of variable thermal conductivity on wave propagation for a ramp-type heating semiconductor magneto-rotator hydrostatic stresses medium during photo-excited microtemperature processes. *Waves Random Complex Media* **2021**, 1–23. [CrossRef]
33. Abbas, I.; Hobiny, A.; Marin, M. Photo-thermal interactions in a semi-conductor material with cylindrical cavities and variable thermal conductivity. *J. Taibah Univ. Sci.* **2020**, *14*, 1369–1376. [CrossRef]
34. Said, S.M.; Othman, M.I.A. The effect of gravity and hydrostatic initial stress with variable thermal conductivity on a magneto-fiber-reinforced. *Struct. Eng. Mech.* **2020**, *74*, 425–434. [CrossRef]
35. Ezzat, M.A.; El-Bary, A.A. Effects of variable thermal conductivity and fractional order of heat transfer on a perfect conducting infinitely long hollow cylinder. *Int. J. Therm. Sci.* **2016**, *108*, 62–69. [CrossRef]
36. Othman, M.I.A.; Abouelregal, A.E. Magnetothermoelstic analysis for an infinite solid cylinder with variable thermal conductivity due to harmonically varying heat. *Microsyst. Technol.* **2017**, *23*, 5635–5644. [CrossRef]
37. Lotfy, K.; Tantawi, R.S.; Anwer, N. Response of Semiconductor Medium of Variable Thermal Conductivity Due to Laser Pulses with Two-Temperature through Photothermal Process. *Silicon* **2019**, *11*, 2719–2730. [CrossRef]
38. Zenkour, A.M.; Abouelregal, A.E. Thermoelastic Interactions in an Infinite Orthotropic Continuum of a Variable Thermal Conductivity with a Cylindrical Hole. *Iran. J. Sci. Technol. Trans. Mech. Eng.* **2017**, *43*, 281–290. [CrossRef]
39. Mahdy, A.M.S.; Lotfy, K.; El-Bary, A.A.; Roshdy, E.M.; Abd El-Raouf, M.M. Variable thermal conductivity during photo-thermoelasticy theory of semiconductor medium induced by laser pulses with hyperbolic two-temperature theory. *Waves Random Complex Media* **2021**, 1–23. [CrossRef]
40. Khamis, A.K.; Lotfy, K.; El-Bary, A.A. Effect of variable thermal conductivity of semiconductor elastic medium during photothermal excitation subjected to thermal ramp type. *Waves Random Complex Media* **2022**, *32*, 78–90. [CrossRef]
41. Khamis, A.K.; El-Bary, A.A.; Lotfy, K. Electromagnetic Hall current and variable thermal conductivity influence for microtemperature photothermal excitation process of semiconductor material. *Waves Random Complex Media* **2022**, *32*, 406–423. [CrossRef]
42. Mandelis, A.; Nestoros, M.; Christofides, C. Thermoelectronic-wave coupling in laser photothermal theory of semiconductors at elevated temperatures. *Opt. Eng.* **1997**, *36*, 459–468. [CrossRef]
43. Song, Y.Q.; Bai, J.T.; Ren, Z.Y. Study on the reflection of photothermal waves in a semiconducting medium under generalized thermoelastic theory. *Acta Mech.* **2012**, *223*, 1545–1557. [CrossRef]
44. Youssef, H.M.; El-Bary, A.A. Theory of hyperbolic two-temperature generalized thermoelasticity. *Mater. Phys. Mech.* **2018**, *40*, 158–171. [CrossRef]
45. Youssef, H. State-space approach on generalized thermoelasticity for an infinite material with a spherical cavity and variable thermal conductivity subjected to ramp-type heating. *Can. Appl. Math. Q.* **2005**, *13*, 4.
46. Abbas, I.A. Generalized magneto-thermoelasticity in a nonhomogeneous isotropic hollow cylinder using the finite element method. *Arch. Appl. Mech.* **2009**, *79*, 41–50. [CrossRef]
47. Abbas, I.A. A two-dimensional problem for a fibre-reinforced anisotropic thermoelastic half-space with energy dissipation. *Sadhana* **2011**, *36*, 411–423. [CrossRef]
48. Das, N.C.; Lahiri, A.; Giri, R.R. Eigenvalue approach to generalized thermoelasticity. *Indian J. Pure Appl. Math.* **1997**, *28*, 1573–1594.
49. Abbas, I.A. A dual phase lag model on thermoelastic interaction in an infinite fiber-reinforced anisotropic medium with a circular hole. *Mech. Based Des. Struct. Mach.* **2015**, *43*, 501–513. [CrossRef]
50. Lahiri, A.; Das, B.; Sarkar, S. Eigenvalue approach to thermoelastic interactions in an unbounded body with a spherical cavity. In Proceedings of the World Congress on Engineering, London, UK, 30 June–2 July 2010; pp. 1881–1886.
51. Crump, K.S. Numerical Inversion of Laplace Transforms Using a Fourier Series Approximation. *J. ACM* **1976**, *23*, 89–96. [CrossRef]
52. Song, Y.Q.; Todorovic, D.M.; Cretin, B.; Vairac, P.; Xu, J.; Bai, J.T. Bending of Semiconducting Cantilevers Under Photothermal Excitation. *Int. J. Thermophys.* **2014**, *35*, 305–319. [CrossRef]